# Searching for Vector Dark Matter with an Optomechanical Accelerometer

Jack Manley [ORCID],[1] Mitul Dey Chowdhury [ORCID],[2] Daniel Grin,[3] Swati Singh,[1] and Dalziel J. Wilson[2,*]

[1]*Department of Electrical and Computer Engineering, University of Delaware, Newark, Delaware 19716, USA*
[2]*Wyant College of Optical Sciences, University of Arizona, Tucson, Arizona 85721, USA*
[3]*Department of Physics and Astronomy, Haverford College, Haverford, Pennsylvania 19041, USA*

We consider using optomechanical accelerometers as resonant detectors for ultralight dark matter. As a concrete example, we describe a detector based on a silicon nitride membrane fixed to a beryllium mirror, forming an optical cavity. The use of different materials gives access to forces proportional to baryon ($B$) and lepton ($L$) charge, which are believed to be coupling channels for vector dark matter particles ("dark photons"). The cavity meanwhile provides access to quantum-limited displacement measurements. For a centimeter-scale membrane precooled to 10 mK, we argue that sensitivity to vector $B - L$ dark matter can exceed that of the Eöt-Wash experiment in integration times of minutes, over a fractional bandwidth of $\sim 0.1\%$ near 10 kHz (corresponding to a particle mass of $10^{-10}$ eV/c$^2$). Our analysis can be translated to alternative systems, such as levitated particles, and suggests the possibility of a new generation of tabletop experiments.

The absence of evidence for dark matter's most popular candidates—WIMPs, axions, and sterile neutrinos—has led to a "growing sense of crisis" in the astronomy community [1]. Unlike gravitational waves, whose recent detection [2] was the culmination of decades of focused effort, the challenge of detecting dark matter (DM) remains complicated by a basic uncertainty of what to look for (for example, the mass of DM particles or objects remains unknown to within 90 orders of magnitude.) In response to this crisis, a growing consensus is advocating a rethinking of DM candidates and the development of a more comprehensive experimental approach [1].

Mechanical DM detectors are of interest for two reasons. First, various models predict that DM produces a force on standard model (SM) particles, for example, a strain due to coupling to fundamental constants [3–5]. Second, advances in the field of cavity optomechanics—largely driven by gravitational wave (GW) astronomy—have seen the birth of a new field of quantum optomechanics, in which high-$Q$ mechanical resonators are probed at the quantum limit using laser fields [6]. This has given access to exquisite force sensitivities over a range of frequencies (1 kHz–10 GHz), which is relatively unexplored, but well motivated, in the search for DM, corresponding to wavelike "ultralight" DM (ULDM).

Here we consider searching for ULDM with optomechanical accelerometers, a technology being pursued in a diversity of platforms ranging from levitated microspheres to whispering gallery mode resonators [7–10]. The concept of accelerometer-based ULDM detection is also well established [11–13], forming the basis for searches based on GW interferometer [14], atom interferometer [15],

and precision torsion-balance experiments [11]. From a theoretical viewpoint, it is motivated by the possibility—conceivable by various production mechanisms [16–26]—that ULDM is composed of a massive vector field [16,17], which could couple to SM through channels such as baryon ($B$) or baryon-minus-lepton ($B - L$) number. This coupling would manifest as an equivalence-principle-violating [11] (material dependent) force on uniform bodies, or a differential acceleration of bodies separated by a distance comparable to the ULDM's de Broglie wavelength.

We wish to emphasize in this Letter that optomechanical accelerometers can also be operated resonantly, enabling high sensitivity at frequencies (1–100 kHz) where current broadband ULDM searches are limited, in a form factor amenable to array-based detection [12]. As an illustration, we consider a detector based on a silicon nitride membrane fixed to a beryllium mirror, forming a Fabry-Pérot cavity (Fig. 1). Through a combination of high mechanical $Q$,
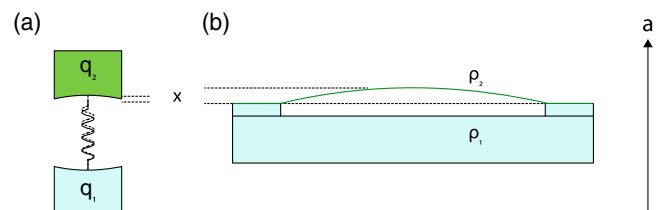


FIG. 1. Concept for an optomechanical accelerometer sensitive to vector $B$ or $B - L$ ultralight dark matter. (a) Lumped-mass model. (b) Membrane-mirror example. Colors represent masses (materials) with different $B$ or $B - L$ charge (charge density), $q_i$ ($\rho_i$).

cryogenic precooling, and quantum-limited displacement readout, we find that this detector can probe vector $B - L$ and $B$ ULDM with sensitivity rivaling the Eöt-Wash experiments [27] in an integration time of minutes, over a fractional bandwidth of $\sim 0.1\%$. Addressing challenges such as frequency tunability (to increase bandwidth) and scalability could enable these and similar optomechanical detectors to occupy a niche in the search for DM.

Before describing the detector, it is useful to recall some basic features of ULDM. First, ultralight refers to particles of mass $m_{DM} \lesssim 1$ eV$/c^2$, which, if virialized within our solar neighborhood (at an average speed of $v_{vir} \sim 10^{-3} c$ [28]) would have a de Broglie wavelength of $\lambda_{DM} = h/(m_{DM} v_{vir}) \gtrsim 1$ mm. Given the local DM energy density, $\rho_{DM} \approx 0.4$ GeV$/$cm$^3$ [29], the number of ULDM particles would be large with a volume $\lambda_{DM}^3$, implying that they behave like a coherent field. This field would oscillate at Compton frequency $\omega_{DM} = m_{DM} c^2 / \hbar \lesssim 2\pi \times 10^{14}$ Hz with a Doppler-broadened linewidth of $\Delta\omega_{DM} = \omega_{DM}(\Delta v_{vir}/c)^2 \sim 10^{-6}\omega_{DM}$. As such, a linear detector for ULDM should look for a narrow-band signal with an effective quality factor of $Q_{DM} = \omega_{DM}/\Delta\omega_{DM} \sim 10^6$. Moreover, terrestrial ULDM detectors should anticipate a spatially uniform signal at frequencies $\omega_{DM} \lesssim 2\pi \times 10$ kHz, for which $\lambda_{DM} \gtrsim 10^4$ km exceeds the radius of the Earth.

The ULDM candidates we focus on are vector (spin-1) bosons, also known as dark photons, coupled to $B - L$ charge. Composing a vector field analogous to an electromagnetic field, $B - L$ dark photons would accelerate free-falling atoms in proportion to their charge-mass (neutron-nucleon) ratio

$$a(t) = g \frac{A - Z}{A} a_0 \cos(\omega_{DM} t + \theta_{DM}), \qquad (1)$$

where $a_0 = 3.7 \times 10^{11}$ m/s$^2$ (see Supplemental Material [30]), $A(Z)$ is the mass (atomic) number, and $g$ is a dimensionless coupling strength. Current constraints from torsion-balance equivalence principle tests (specifically, the Eöt-Wash experiments [27]) imply $g \lesssim 10^{-22}$ for $\omega_{DM} \lesssim 2\pi \times 10$ kHz. To exceed this bound, it is necessary to resolve accelerations at the level of

$$\sqrt{S_{aa}} \sim g a_0 \sqrt{\frac{Q_{DM}}{\omega_{DM}}} \lesssim 10^{-11} \sqrt{\frac{10 \text{ kHz}}{\omega_{DM}/2\pi}} \frac{g_0}{\sqrt{\text{Hz}}} \qquad (2)$$

($g_0 = 9.8$ m/s$^2$), a task which is extreme for most accelerometers because it requires a displacement sensitivity of

$$\sqrt{S_{xx}} = \frac{\sqrt{S_{aa}}}{\omega_{DM}^2} \lesssim 10^{-20} \sqrt{\left(\frac{10 \text{ kHz}}{\omega_{DM}/2\pi}\right)^5} \frac{\text{m}}{\sqrt{\text{Hz}}}. \qquad (3)$$

Optomechanical accelerometers employ a mechanical resonator as a test mass and an optical cavity for displacement-based readout. To illustrate how this can be used to detect dark photons, we first consider a lumped-mass model [Fig. 1(a)], in which two mirrors made of different materials, forming a cavity of length $L \ll \lambda_{DM}$, are attached by a massless spring. Dark photons would produce a *differential* mirror acceleration

$$a(t) = g f_{12} a_0 \cos(\omega_{DM} t + \theta_{DM}), \qquad (4)$$

where $f_{12}$ is a purely material-dependent suppression factor

$$f_{12} = \left| \frac{Z_1}{A_1} - \frac{Z_2}{A_2} \right|. \qquad (5)$$

The resulting cavity length change $x$, which is the experimental observable, can be expressed in spectral density units as

$$S_{xx}[\omega] = \frac{1}{(\omega^2 - \omega_0^2)^2 + \omega_0^2 \omega^2 / Q_0^2} S_{aa}[\omega], \qquad (6)$$

where $\omega_0$ and $Q_0$ are the frequency and quality factor of the mass-spring system, respectively.

The advantage of the optomechanical approach is two-fold. First, cavity enhanced readout can achieve high displacement sensitivities—an extreme case being the Laser Interferometer Gravitational-Wave Observatory (LIGO), which has achieved sensitivities of $10^{-20}$ m$/\sqrt{\text{Hz}}$ at $\omega \sim 2\pi \times 100$ Hz, sufficient to satisfy Eq. (3) [14]. Second, displacement sensitivity requirements are relaxed on resonance by a factor of $Q_0$, giving access to thermal-noise-limited acceleration sensitivities [8,10]

$$S_{aa}^{\text{th}} = \frac{4 k_B T \omega_0}{m Q_0}, \qquad (7)$$

where $T$ ($m$) is the resonator temperature (effective mass). While resonant operation is not typically exploited in optomechanical accelerometers, $\sqrt{S_{aa}^{\text{th}}} < 10^{-11} \, g_0/\sqrt{\text{Hz}}$ might be realized in a variety of current platforms translated to cryogenic temperatures. The trade-off, as is well known, is a $Q_0$-fold reduction in bandwidth, such that the sensitivity-bandwidth product is (in the ideal case of $T = 0$) preserved.

Modern cavity optomechanical systems provide numerous platforms for realizing an ULDM detector. As an illustration, we consider the system sketched in Fig. 1(b), consisting of a silicon nitride (Si$_3$N$_4$) membrane rigidly attached to a beryllium (Be) mirror. It bears emphasis that special care must be taken to ensure that such an extended system is faithful to the lumped-mass model. In particular, the use of different materials [represented by charge densities $\rho_i$ in Fig. 1(b)] is necessary to ensure that the suppression factor $f_{12}$ is nonzero ($f_{12} = 0.053$ for Si$_3$N$_4$-Be). The system must also be placed in free fall.
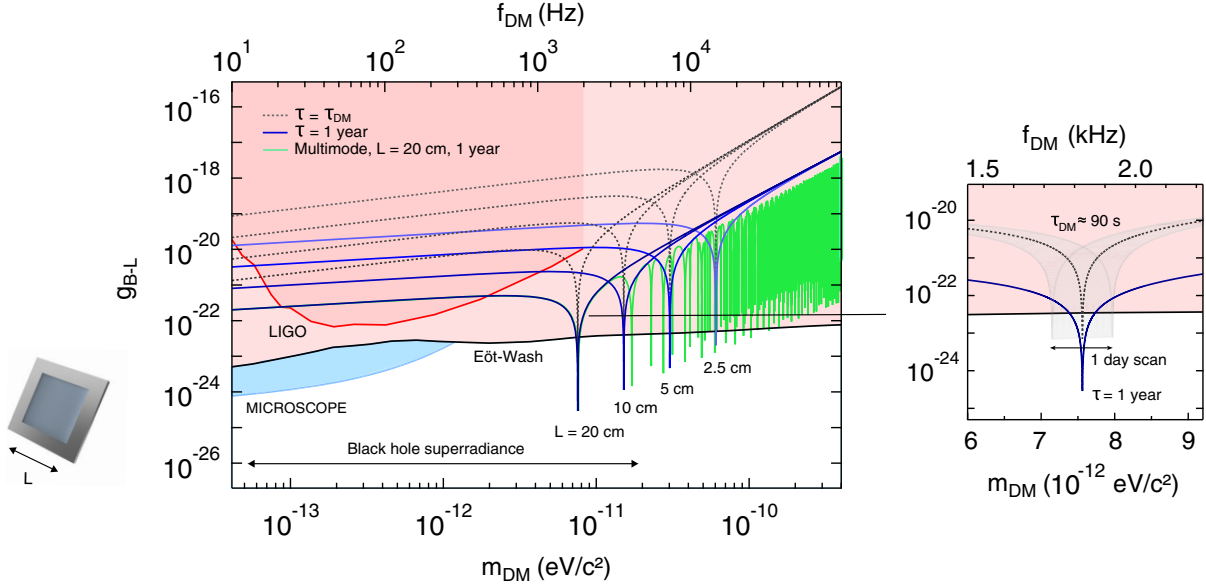
FIG. 2. Centimeter-scale $Si_3N_4$ membranes as vector $B - L$ dark matter detectors. Dashed gray and solid blue curves are models for the acceleration sensitivity of four different membranes, expressed as a minimum $B - L$ coupling strength $g_{B-L}$ [Eq. (12)], for a measurement time equal to the DM coherence time ($\tau_{DM} = 2Q_{DM}/\omega_{DM}$) and one year, respectively. Each model assumes a mechanical quality factor of $Q_0 = 10^9$, an operating temperature of $T = 10$ mK, a displacement sensitivity of $2 \times 10^{-17}$ m/$\sqrt{Hz}$, and a suppression factor of $f_{12} = 0.05$ relative to a Be reference mass. A full multimode spectrum for the 20 cm membrane is shown in green. Pink, red, and blue regions are bounds set by the Eöt-Wash experiments, LIGO, and MICROSCOPE, respectively. At right, we zoom in on the resonance of the 20 cm membrane and illustrate a day-long scan (gray region) made in intervals $\tau_{DM} \approx 1.5$ min with a step size equal to the detection bandwidth $\Delta\omega_{det} \approx 2\pi \times 0.2$ Hz.

This can be simulated, for example, by suspending the device from a pendulum with corner frequency $\ll \omega_0$.

The use of a $Si_3N_4$ membrane is motivated by a set of features that represent the generic strengths of modern optomechanical devices and several that make them specifically compelling for on-resonance accelerometry. Among these are the ability to achieve ultrahigh-quality factors, approaching one billion, using phononic engineering [49,50]; the ability to tune resonance frequencies (to enhance bandwidth) using radiation pressure [51], thermal [52,53], and electrostatic forces [54]; parts-per-million optical loss [55]; and the ability to operate as a high reflectivity mirror by photonic crystal (PtC) patterning [56,57]. Specific to accelerometry, a peculiar feature of membranes is their $Q_0$ versus mass scaling: due to an effect called dissipation dilution [50], the $Q_0$ of tensily stressed membranes increases with their area, enabling large $Q_0 \times m$ factors in a relatively compact (in one dimension) form factor.

We thus envision, without loss of generality, a finesse $\mathcal{F} = 100$ cavity formed by a Be mirror and a 200-nm-thick $Si_3N_4$ membrane with an embedded PtC micromirror [57]. Probed by a coherent laser (power $P$, wavelength $\lambda$) using an ideal homodyne receiver, the detector output can be modeled as

$$S_{xx}^{tot} = S_{xx}^{imp} + |\chi_{xa}(\omega)|^2(S_{aa}^{ba} + S_{aa}^{th} + S_{aa}^{DM}), \quad (8)$$

where

$$S_{xx}^{imp} = \frac{\pi\hbar c\lambda}{64\mathcal{F}^2 P} \quad (9)$$

is the apparent displacement (imprecision) due to laser phase shot noise [6,30],

$$S_{aa}^{ba} = \frac{\hbar^2}{m^2 S_{xx}^{imp}} \quad (10)$$

is the acceleration (backaction) due to radiation pressure shot noise (see Supplemental Material [30]), and $\chi_{xa}[\omega] = (\omega^2 - \omega_0^2 + i\omega_0^2/Q_0)^{-1}$ is the mechanical susceptibility (here assuming structural damping [58]).

In essence, ULDM detection is a parameter estimation problem. To estimate $g$, we model the dark photon signal ($a_{DM}$) as a Lorentzian noise peak [30]

$$S_{aa}^{DM}[\omega_{DM}] \approx \frac{4\langle a_{DM}^2\rangle}{\Delta\omega_{DM}} \approx \frac{2}{3}(\beta g f_{12} a_0)^2 \frac{Q_{DM}}{\omega_{DM}}, \quad (11)$$

here assuming a randomly polarized DM field ($\langle a^2\rangle \rightarrow \langle a^2\rangle/3$) and introducing a spatial overlap factor $\beta = (4/\pi)^2$ for the fundamental membrane mode [30]. By feedback damping [59,60] or optimal filtering [60–62], the narrow transfer function $|\chi_{xa}|^2$ can be inverted from the detector signal and $S_{aa}^{DM}[\omega_{DM}]$ can be estimated, for

example, by averaging periodograms [30]. Equating $S_{aa}^{DM}[\omega_{DM}]$ with the variance in the detector noise $S_{aa}^{det}[\omega] = |\chi_{xa}(\omega)|^{-2}S_{xx}^{imp} + (S_{aa}^{ba} + S_{aa}^{th})$ yields a lower bound of [30,63]

$$g_{min}[\omega] = \frac{\sqrt{3}}{\beta f_{12}a_0}\sqrt{\frac{S_{aa}^{det}[\omega]}{\tau_{DM}}} \times \begin{cases} \left(\frac{\tau_{DM}}{\tau}\right)^{1/2} & \tau \lesssim \tau_{DM} \\ \left(\frac{\tau_{DM}}{\tau}\right)^{1/4} & \tau \gg \tau_{DM}, \end{cases} \quad (12a)$$

$$\geq \frac{\sqrt{3/2}}{\beta f_{12}a_0}\sqrt{\frac{4k_B T\omega_{DM}^2}{mQ_0Q_{DM}}} \times \begin{cases} \left(\frac{\tau_{DM}}{\tau}\right)^{1/2} & \tau \lesssim \tau_{DM} \\ \left(\frac{\tau_{DM}}{\tau}\right)^{1/4} & \tau \gg \tau_{DM}, \end{cases} \quad (12b)$$

where $\tau_{DM} = 2Q_{DM}/\omega_{DM}$ and $\tau$ are the DM coherence time and total measurement time, respectively.

In Fig. 2, we plot $g_{min}$ for the fundamental mode of square membranes ranging from 2.5 to 20 cm wide, with resonance frequencies spanning from 2 to 25 kHz. We assume $Q_0 = 10^9$, $T = 10$ mK, $\lambda = 1$ $\mu$m, and $P = 0.3$ mW, corresponding to a displacement sensitivity of $\sqrt{S_{xx}^{imp}} \approx 2 \times 10^{-17}$ m/$\sqrt{Hz}$. We compare measurements spanning the dark matter coherence time $\tau = \tau_{DM} \sim$ 10–100 sec (dashed gray curves) to measurements spanning one year (blue curves) and find that bounds set by the Eöt-Wash experiments can be exceeded by more than an order of magnitude. Comparison is made to recent constraints from LIGO in its 10 Hz–1 kHz detection band (red curve) [14]. Despite the large difference in displacement sensitivity between LIGO and our model system, the main difference is that LIGO's test masses are made of the same material, so that differential acceleration is produced only by the field gradient ($f_{12} \approx \pi L/\lambda_{DM} \sim 10^{-4} - 10^{-6}$, see Supplemental Material [30]).

Interestingly, the bandwidth and sensitivity of our model detector is limited by quantum backaction [12]. To visualize this trade-off, in Fig. 3 we focus on the "10 cm" peak in Fig. 2 and vary the optical power between 0.1 and 10 mW. At 0.1 mW, thermal and backaction noise are equivalent, and the detection bandwidth ($\Delta\omega_{det}$) corresponds to the frequency range over which the total motion is resolved ($S_{xx}^{imp} < S_{xx}^{th} + S_{xx}^{ba}$). At higher powers, bandwidth is increased proportionately; however, sensitivity is simultaneously reduced due to quantum backaction ($S_{xx}^{ba} > S_{xx}^{th}$). This well-known limit to the sensitivity-bandwidth product corresponds to the standard quantum limit for a force measurement, illustrated by the pink lines in Fig. 3. In our example, evidently, maintaining sensitivity below the Eöt-Wash bound ($g \sim 10^{-22}$) requires limiting the fractional detection bandwidth to $\Delta\omega_{det}/\omega_0 \sim 10\%$.

Several techniques could improve the bandwidth of optomechanical DM detectors. For example, a "xylophone" detector could be realized by simultaneously monitoring multiple higher-order modes, taking advantage of the
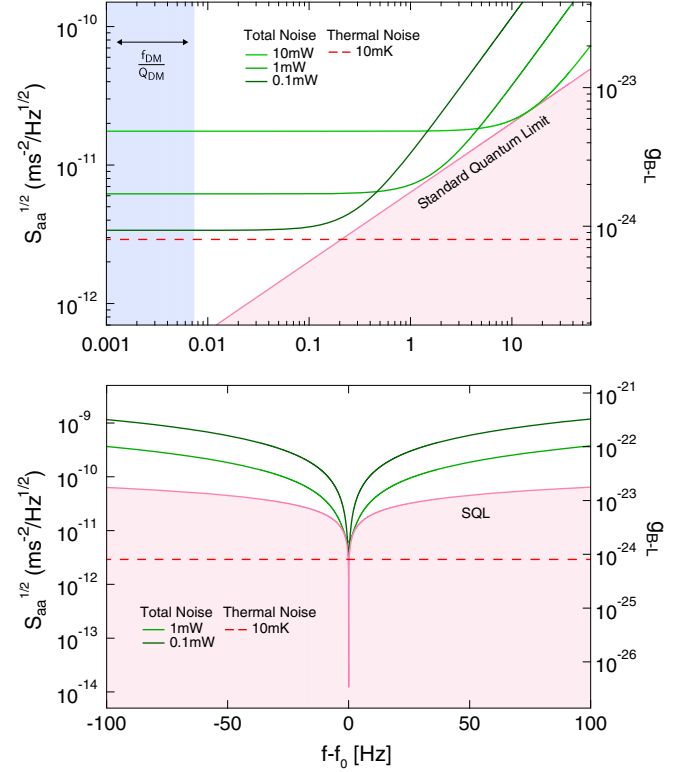


FIG. 3. Detector sensitivity near resonance, versus optical power, for the 10 cm membrane in Fig. 2, indicating sensitivity-bandwidth trade-offs due to thermal, backaction, and imprecision noise. Log-log (top) and log-linear (bottom) plots are shown for emphasis. The standard quantum limit (pink line) is achieved when backaction and imprecision noise are equal and can dominate thermal noise (dotted red line) off resonance. The width of ULDM signal is shaded blue.

high bandwidth of optical readout. [In our case, a $L \sim 1$ mm cavity length would yield a readout bandwidth of $c/(2L\mathcal{F}) \sim 1$ GHz, encompassing $\sim 10^{11}$ modes of a 10 cm membrane.] A full multimode spectrum [30], shown as a green curve in Fig. 2, indicates that a single membrane can in this way yield the same performance as an array of (single mode) membranes with different sizes. A more direct approach, similar to axion haloscope experiments [64], would be to sweep the mechanical resonance frequency. Considering the reduced efficiency of signal averaging for times $\tau > \tau_{DM}$ [Eq. (12)], a natural strategy would be to step in intervals of the detection bandwidth $\Delta\omega_{det}$ for a total of $N = \tau/\tau_{DM}$ steps. For the 10 cm example in Fig. 2, this approach would yield an octave (a fractional bandwidth of $\Delta\omega_{det}N/\omega_0 = 100\%$) in $\tau \sim Q_{DM}/\Delta\omega_{det} \sim 1$ week. Since membrane frequency scanning methods [51–54] are typically limited to $\sim 10\%$ fractional bandwidth, realizing a broadband detector might in practice require a combination of xylophone, scanning, and array-based techniques. For example, an array of 10 membranes as shown in Fig. 2, appropriately separated in resonance frequency from 2 to 4 kHz, and capable of $10\%$
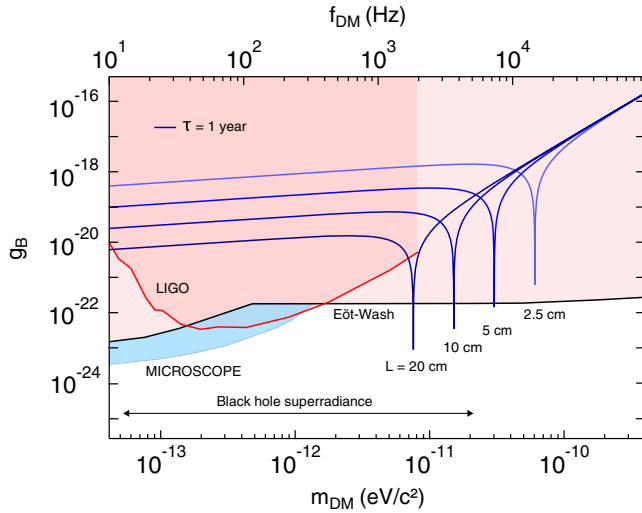
FIG. 4. Projected sensitivity to $B$-coupled dark photons. Blue curves are for centimeter-scale membranes as in Fig. 2, with the suppression factor $f_{12}$ adjusted for $B$ coupling. Black, red, and light blue curves are constraints set by the Eöt-Wash experiments, LIGO, and MICROSCOPE experiments, respectively.

fractional sweeps, could allow for an effectively broadband, thermal-noise-limited search above $\omega_{DM} > 2\pi \times 1$ kHz, exceeding Eöt-Wash bounds between 2 and 20 kHz in approximately 1 week. [In motivating such a search, it is interesting to note that $\omega_{DM} = 2\pi \times (1-10)$ kHz dark photons, besides having well-motivated production mechanisms [16–25], can be independently constrained by black hole population statistics, since the corresponding Compton wavelength is comparable to the event horizon of stellar-mass black holes [65–68].]

Finally, we point out that the differential accelerometer approach is not limited to $B - L$ coupling. For example, $B$-coupled dark photons, for which $f_{12} = |A_1/\mu_1 - A_2/\mu_2|$ [30], where $\mu_i$ is the mass in atomic mass units, would give rise to a differential acceleration between SiN and Be with a suppression factor of $f_{12} = 0.0018$. In Fig. 4, we plot the predicted sensitivity of our detector to $B$-coupled dark photons compared to the constraints set by the Eöt-Wash experiments [69], LIGO [14], and MICROSCOPE [70,71], suggesting a similar advantage at 1–10 kHz Compton frequencies.

In summary, we have discussed the use of optomechanical accelerometers as resonant detectors for ULDM, focusing on $B$- or $B - L$-coupled dark photons, which produce an oscillating acceleration between masses made of different materials. We considered an example based on a centimeter-scale $Si_3N_4$ membrane coupled to a Be mirror and argued that, by combining quantum-limited displacement readout with cryogenic operating temperatures, the sensitivity of this detector can exceed current bounds, set by the Eöt-Wash experiments, in measurement time of minutes, over a fractional bandwidth of $\sim 0.1\%$ in the mass range $10^{-11}$–$10^{-10}$ eV/c$^2$. We also described scanning

techniques that could broaden the bandwidth of this detector to more than an octave. Looking forward, we anticipate that a variety of optomechanical accelerometer platforms can perform similarly as vector ULDM detectors. Optically or magnetically levitated test masses seem particularly promising, as in addition to ultrahigh-$Q_0 \times m$ factors, they can be frequency scanned over a wide bandwidth [7,72,73].

*Corresponding author.
dalziel.wilson@gmail.com

[1] G. Bertone and T. M. Tait, Nature (London) **562**, 51 (2018).
[2] B. P. Abbott, R. Abbott, T. Abbott, M. Abernathy, F. Acernese, K. Ackley, C. Adams, T. Adams, P. Addesso, R. Adhikari et al., Phys. Rev. Lett. **116**, 061102 (2016).
[3] T. Damour and J. F. Donoghue, Phys. Rev. D **82**, 084033 (2010).
[4] A. Arvanitaki, S. Dimopoulos, and K. Van Tilburg, Phys. Rev. Lett. **116**, 031102 (2016).
[5] J. Manley, D. J. Wilson, R. Stump, D. Grin, and S. Singh, Phys. Rev. Lett. **124**, 151301 (2020).
[6] M. Aspelmeyer, T. J. Kippenberg, and F. Marquardt, Rev. Mod. Phys. **86**, 1391 (2014).
[7] F. Monteiro, S. Ghosh, A. G. Fine, and D. C. Moore, Phys. Rev. A **96**, 063841 (2017).
[8] F. Guzmán Cervantes, L. Kumanchik, J. Pratt, and J. M. Taylor, Appl. Phys. Lett. **104**, 221111 (2014).
[9] Y. L. Li and P. Barker, J. Lightwave Technol. **36**, 3919 (2018).
[10] A. G. Krause, M. Winger, T. D. Blasius, Q. Lin, and O. Painter, Nat. Photonics **6**, 768 (2012).
[11] P. W. Graham, D. E. Kaplan, J. Mardon, S. Rajendran, and W. A. Terrano, Phys. Rev. D **93**, 075029 (2016).
[12] D. Carney, A. Hook, Z. Liu, J. M. Taylor, and Y. Zhao, arXiv:1908.04797.
[13] A. Pierce, K. Riles, and Y. Zhao, Phys. Rev. Lett. **121**, 061102 (2018).
[14] H.-K. Guo, K. Riles, F.-W. Yang, and Y. Zhao, Commun. Phys. **2**, 155 (2019).
[15] A. A. Geraci and A. Derevianko, Phys. Rev. Lett. **117**, 261301 (2016).
[16] A. E. Nelson and J. Scholtz, Phys. Rev. D **84**, 103501 (2011).
[17] P. Arias, D. Cadamuro, M. Goodsell, J. Jaeckel, J. Redondo, and A. Ringwald, J. Cosmol. Astropart. Phys. 06 (2012) 013.
[18] P. W. Graham, J. Mardon, and S. Rajendran, Phys. Rev. D **93**, 103520 (2016).
[19] J. Cembranos, A. Maroto, and S. J. Nez Jareo, J. High Energy Phys. 02 (2017) 064.

[20] J. A. Dror, K. Harigaya, and V. Narayan, Phys. Rev. D **99**, 035036 (2019).

[21] R. T. Co, A. Pierce, Z. Zhang, and Y. Zhao, Phys. Rev. D **99**, 075002 (2019).

[22] M. Bastero-Gil, J. Santiago, L. Ubaldi, and R. Vega-Morales, J. Cosmol. Astropart. Phys. 04 (2019) 015.

[23] P. Agrawal, N. Kitajima, M. Reece, T. Sekiguchi, and F. Takahashi, Phys. Lett. B **801**, 135136 (2020).

[24] K. Nakayama, J. Cosmol. Astropart. Phys. 10 (2019) 019.

[25] K. Nomura, A. Ito, and J. Soda, Eur. Phys. J. C **80**, 419 (2020).

[26] Y. Nakai, R. Namba, and Z. Wang, J. High Energy Phys. 12 (2020) 170.

[27] T. A. Wagner, S. Schlamminger, J. H. Gundlach, and E. G. Adelberger, Classical Quantum Gravity **29**, 184002 (2012).

[28] K. Freese, M. Lisanti, and C. Savage, Rev. Mod. Phys. **85**, 1561 (2013).

[29] M. Tanabashi, K. Hagiwara, K. Hikasa, K. Nakamura, Y. Sumino, F. Takahashi, J. Tanaka, K. Agashe, G. Aielli, C. Amsler *et al.*, Phys. Rev. D **98**, 030001 (2018).

[30] See Supplemental Material at http://link.aps.org/supplemental/10.1103/PhysRevLett.126.061301 for further information on vector dark matter and the proposed detection strategy, which includes Refs. [31–48].

[31] D. J. E. Marsh, Phys. Rep. **643**, 1 (2016).

[32] A. Arvanitaki, S. Dimopoulos, S. Dubovsky, N. Kaloper, and J. March-Russell, Phys. Rev. D **81**, 123530 (2010).

[33] D. B. Kaplan and M. B. Wise, J. High Energy Phys. 08 (2000) 037.

[34] B. de Carlos, J. A. Casas, F. Quevedo, and E. Roulet, Phys. Lett. B **318**, 447 (1993).

[35] J. P. Conlon, J. High Energy Phys. 05 (2006) 078.

[36] E. Witten, Phys. Lett. **149B**, 351 (1984).

[37] P. Svrcek and E. Witten, J. High Energy Phys. 06 (2006) 051.

[38] T. R. Taylor and G. Veneziano, Phys. Lett. B **213**, 450 (1988).

[39] M. Cicoli, Proc. Sci. EPS-HEP2011 (**2011**) 127.

[40] T. Damour and A. M. Polyakov, Gen. Relativ. Gravit. **26**, 1171 (1994).

[41] T. Damour, F. Piazza, and G. Veneziano, Phys. Rev. Lett. **89**, 081601 (2002).

[42] C. P. Burgess, A. Maharana, and F. Quevedo, J. High Energy Phys. 05 (2011) 010.

[43] T. Damour and A. M. Polyakov, Nucl. Phys. **B423**, 532 (1994).

[44] M. Cicoli, M. Goodsell, and A. Ringwald, J. High Energy Phys. 10 (2012) 146.

[45] B. S. Acharya, K. Bobkov, and P. Kumar, J. High Energy Phys. 11 (2010) 105.

[46] H. Ruegg and M. Ruiz-Altaba, Int. J. Mod. Phys. A **19**, 3265 (2004).

[47] M. Schambach and K. Sanders, Rep. Math. Phys. **82**, 203 (2018).

[48] A. Derevianko, Phys. Rev. A **97**, 042506 (2018).

[49] Y. Tsaturyan, A. Barg, E. S. Polzik, and A. Schliesser, Nat. Nanotechnol. **12**, 776 (2017).

[50] A. H. Ghadimi, S. A. Fedorov, N. J. Engelsen, M. J. Bereyhi, R. Schilling, D. J. Wilson, and T. J. Kippenberg, Science **360**, 764 (2018).

[51] N. Flowers-Jacobs, S. Hoch, J. Sankey, A. Kashkanova, A. Jayich, C. Deutsch, J. Reichel, and J. Harris, Appl. Phys. Lett. **101**, 221109 (2012).

[52] R. St-Gelais, S. Bernard, C. Reinhardt, and J. C. Sankey, ACS Photonics **6**, 525 (2019).

[53] P. Sadeghi, M. Tanzer, N. Luhmann, M. Piller, M.-H. Chien, and S. Schmid, Phys. Rev. Applied **14**, 024068 (2020).

[54] S. Naserbakht, A. Naesby, and A. Dantan, Appl. Sci. **9**, 4845 (2019).

[55] J. Steinlechner, C. Krüger, I. W. Martin, A. Bell, J. Hough, H. Kaufer, S. Rowan, R. Schnabel, and S. Steinlechner, Phys. Rev. D **96**, 022007 (2017).

[56] J. P. Moura, R. A. Norte, J. Guo, C. Schäfermeier, and S. Gröblacher, Opt. Express **26**, 1895 (2018).

[57] X. Chen, C. Chardin, K. Makles, C. Caër, S. Chua, R. Braive, I. Robert-Philip, T. Briant, P.-F. Cohadon, A. Heidmann *et al.*, Light Sci. Appl. **6**, e16190 (2017).

[58] P. R. Saulson, Phys. Rev. D **42**, 2437 (1990).

[59] E. Gavartin, P. Verlot, and T. J. Kippenberg, Nat. Nanotechnol. **7**, 509 (2012).

[60] G. I. Harris, D. L. McAuslan, T. M. Stace, A. C. Doherty, and W. P. Bowen, Phys. Rev. Lett. **111**, 103603 (2013).

[61] P. Astone, P. Bonifazi, and G. Pallottino, Rev. Sci. Instrum. **61**, 3899 (1990).

[62] A. Pontin, M. Bonaldi, A. Borrielli, F. S. Cataliotti, F. Marino, G. A. Prodi, E. Serra, and F. Marin, Phys. Rev. A **89**, 023848 (2014).

[63] D. Budker, P. W. Graham, M. Ledbetter, S. Rajendran, and A. O. Sushkov, Phys. Rev. X **4**, 021030 (2014).

[64] T. Braine, R. Cervantes, N. Crisosto, N. Du, S. Kimes, L. Rosenberg, G. Rybka, J. Yang, D. Bowring, A. Chou *et al.*, Phys. Rev. Lett. **124**, 101303 (2020).

[65] R. Brito, V. Cardoso, and P. Pani, Lect. Notes Phys. **906**, 1 (2015).

[66] V. Cardoso, P. Pani, and T.-T. Yu, Phys. Rev. D **95**, 124056 (2017).

[67] M. Baryakhtar, R. Lasenby, and M. Teo, Phys. Rev. D **96**, 035019 (2017).

[68] V. Cardoso, s. J. C. Dias, G. S. Hartnett, M. Middleton, P. Pani, and J. E. Santos, J. Cosmol. Astropart. Phys. 03 (2018) 043.

[69] S. Schlamminger, K.-Y. Choi, T. A. Wagner, J. H. Gundlach, and E. G. Adelberger, Phys. Rev. Lett. **100**, 041101 (2008).

[70] P. Touboul, G. Métris, M. Rodrigues, Y. André, Q. Baghi, J. Bergé, D. Boulanger, S. Bremer, P. Carle, R. Chhun *et al.*, Phys. Rev. Lett. **119**, 231101 (2017).

[71] J. Bergé, P. Brax, G. Métris, M. Pernot-Borràs, P. Touboul, and J.-P. Uzan, Phys. Rev. Lett. **120**, 141101 (2018).

[72] C. W. Lewandowski, T. D. Knowles, Z. B. Etienne, and B. D'Urso, arXiv:2002.07585.

[73] C. Timberlake, G. Gasbarri, A. Vinante, A. Setter, and H. Ulbricht, Appl. Phys. Lett. **115**, 224101 (2019).